

# Antiviral activity of vinifera leaf

Subjects: Virology

Contributor: Aldo Manzin

*Vitis vinifera* represents an important and renowned source of compounds with significant biological activity. Wines and winery bioproducts, such as grape pomace, skins, and seeds, are rich in bioactive compounds against a wide range of human pathogens, including bacteria, fungi, and viruses. However, little is known about the biological properties of vine leaves.

Keywords: HSV-1 ; antiviral ; antimicrobial ; *Vitis vinifera* ; leaf extract ; natural extract ; flavonoids ; molecular networking ; LC-MS

---

## 1. Introduction

Grapevine is one of the major fruit crops worldwide, in terms of economic value and cultivated area. A large amount is subjected to wine production; however, grape has become a model for molecular biology, genetics, and breeding, garnering significant research interest in different areas from the study of polyphenols [1][2][3] to the investigation of specific gene families, such as resistant genes [4].

Grapevine is a plant rich in bioactive compounds [5][6], known for its therapeutic effects. The grape extract was studied for a long time for its hepatoprotective [7], hypoglycemic [8], cardio-protective [9], antioxidant [10][11], antibacterial [11][12][13], and antiviral activity [11][14] which are due to the high levels of polyphenolic compounds found in grapes skin, seeds, and stem. The anti-cancer effect, that has long been studied over the years, is attributable to the consistent antioxidant activity of these molecules [15][16]. Resveratrol, for example, one of the most abundant molecules in the extracts, acts at various levels of carcinogenesis [17]. Grape seed extract inhibits the expression of the epidermal growth factor receptor (EGFR) in head and neck cutaneous squamous cell carcinoma [18], and of MEK/ERK1-2 and MAPK/p38 in breast cancer, counteracting tumor invasiveness and progression. Some phenolic compounds, such as quercetin and catechins, given their similarity to estrogenic hormones, determine a pro- and anti-estrogenic receptor response in breast cancer [19]. Sharma et al. demonstrated the apoptotic activity of proanthocyanidins blocking COX-2 and the prostaglandin receptor (PGE2) [20]. In this context, two stilbenoids of wine, trans-astringin and trans-piceatannol, also show a cancer-chemiopreventive action by inhibiting cyclooxygenases and precancerous lesions [21]. Recently, Di Meo et al. evaluated the anti-cancer activity of grape seeds semi-polar extracts of two Italian grape varieties (Aglianico and Falanghina). They found that the extracts of both varieties are able to inhibit growth and migration of three different mesothelioma cell lines by activating apoptosis [22].

Antibacterial activity has widely been reported [23][24][25][26][27][28]. Anđelković et al. [29] demonstrated that flavonols, phenolic acids, and flavan-3-ols were the main components of grape leaf extracts driving antioxidant and antibacterial activity, principally inhibiting Gram-positive bacteria. A similar effect has been observed by Rodríguez-Vaquero et al. [30], who analyzed the antimicrobial potential of three Argentinian wines: *Listeria monocytogenes* growth was highly reduced by caffeic acid, rutin, and quercetin. Instead, Papadopoulou et al. [31] reported that alcohol-free red and white wine extracts also had antimicrobial potential against *Escherichia coli* and *Candida albicans*, albeit it was less strong than that observed against *Staphylococcus aureus*.

## 2. Antiviral Activity of *Vitis vinifera* Leaf Extract against SARS-CoV-2 and HSV-1

### 2.1. Flavonoid Composition of *V. vinifera* Leaves

Negative ionization mode HPLC-MS/MS is one of the powerful methods to characterize flavonoids because it provides information on both aglycones and glycosidic conjugates that can differentiate isomers [32][33]. HPLC-MS/MS IDA analysis was carried out to investigate *V. vinifera* leaves metabolic profile.

MZmine [34] and GNPS [35] software were used to convert and analyze the raw MS data, and finally Cytoscape built the complex network shown in **Figure 1**. Each node indicates a precursor ion, the node size is strongly related to its abundance in the sample (sum precursor intensity), and the edges size between two nodes is directly dependent on their MS/MS spectra similarity (cosine score) [36]. Analysis of GNPS results together with data manual curation evidenced the presence in the network of one big flavonoids cluster together with a smaller one belonging to digalactosylmonoacylglycerol (DGMG) lipids; other unpaired nodes have also been identified during GNPS analysis (**Figure 1**).

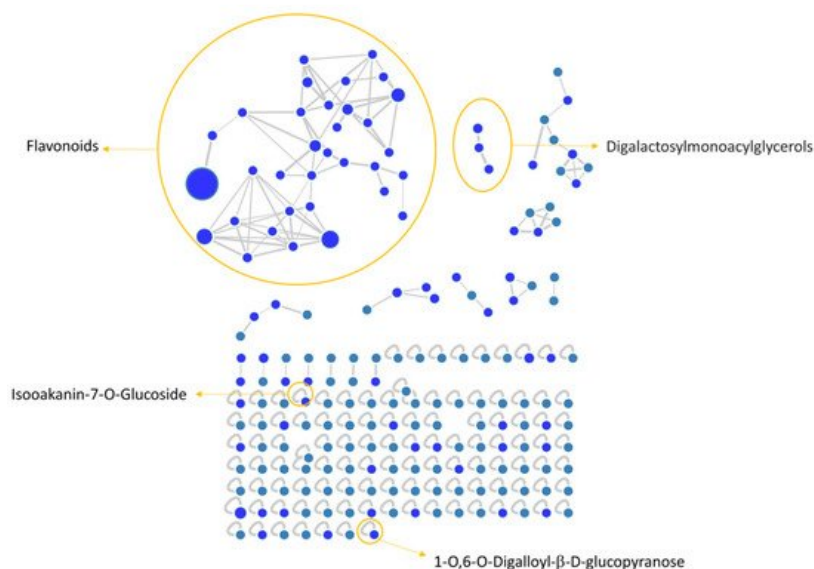


**Figure 1.** *V. vinifera* extract Feature Based Molecular Network (FBMN) obtained through GNPS analysis and Cytoscape visualization, displaying the presence of flavonoids and digalactosylmonoacylglycerol clusters, together with two unpaired nodes matching with 1-O,6-O-Digalloyl-β-D-glucopyranose and Isookanin-7-O-glucoside.

Assignment of each node has been manually curated and the putative identification is reported, Results showed that compound **1** was not in a cluster and it was identified by the GNPS annotation tool as the tannin 1-O,6-O-Digalloyl-β-D-glucopyranose.

A detailed analysis of the MS and MS<sup>2</sup> spectra, combined with the GNPS annotation tools, lead to the characterization of 35 flavonoids conjugates. Most of them were quercetin derivatives (8 compounds), others included derivatives of luteolin (5 compounds), kaempferol (4 compounds), apigenin (3 compounds), isorhamnetin (2 compounds), myricetin, chrysoeriol, biochanin, isookanin, and scutellarein (1 compound) (**Figure 2**). Four flavonoids were not identified (N.I.).

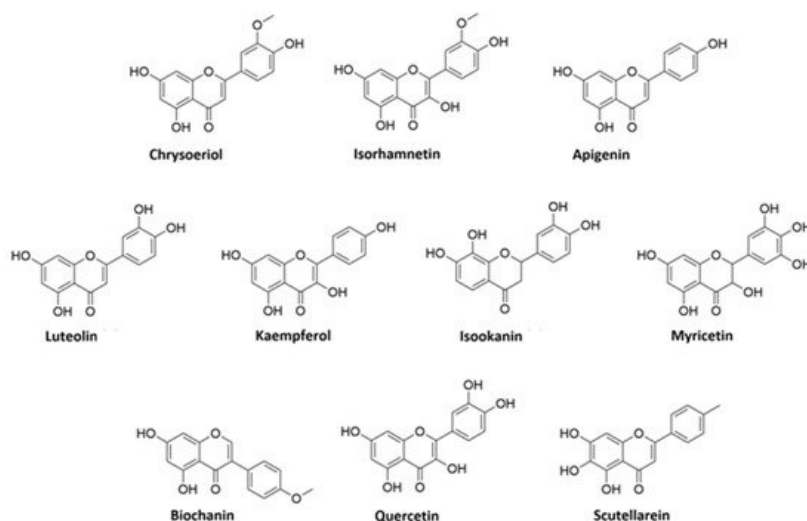


**Figure 2.** Structures of flavonoid aglycones identified in *V. vinifera*.

Moreover, we calculated the relative abundance of each compound present in **Table 2** within the same chemical class. Results showed that compound **13** is the most representative among polyphenols, accounting for more than 44% of the total, followed by compounds **6** and **11**, with 16% and 13%, respectively. Compounds **8**, **14**, **15**, **26**, and **28** account for

less than 10% each, while all the others are present in less than 1% or traces. Among DGMGs, compound **37** is the most representative, with 97%, while compound **38** is present in traces and compound **39** represents 3% of the cluster.

## 2.2. Identification of Kaempferol and Luteolin Derivatives

The aglycone fragment at  $m/z$  285 of compounds **2**, **20**, **23**, **25**, and **26** suggested that they originated from kaempferol or luteolin. Compounds **2**, **20**, and **26** produced a pseudo molecular ion at  $m/z$  447  $[M - H]^-$ , and the  $MS^2$  profile showed typical fragments of hexose glycoside flavone, as they exhibited peaks at  $m/z$  357  $[M - H-90]^-$ , 327  $[M - H-120]^-$ , and 297  $[M - H-150]^-$ . Thus, based on the  $MS^2$  fragmentation profile and RT, compound **2** could be assigned as kaempferol-8-C-glucoside, compound **20** as kaempferol-7-O-glucoside, and compound **26** as kaempferol-3-O-glucoside [33][37][38].

Compound **23**,  $m/z$  593, is characterized by the neutral loss (NL) of (rhamnosyl-hexoside) moiety  $[M - H-308]^-$ , and by comparison of its  $MS^2$  pattern with the literature, we assigned the identity as kaempferol-3-O-(6-O-rhamnosyl-galactoside) [39]. Compound **25** showed the NL of a glucuronide unit  $[M - H-176]^-$  and it was assigned as kaempferol-3-O-glucuronide.

Compounds **4**, **6**, **8**, **9**, and **18** are characterized by the presence of aglycone fragment at  $m/z$  285 and they are all isomers with a parental ion at  $m/z$  447  $[M - H]^-$ . These isomers were identified through the GNPS database and discriminated by RT as orientin, isoorientin, luteolin-4-O-glucoside, and ymaroside, respectively. Differently, compound **24** showed parental ion at  $m/z$  483 and was generally assigned as luteolin-C-hexoside, by comparison with a precedent study [40].

## 2.3. Identification of Apigenin Derivatives

Compounds **10**, **11**, and **29** exhibited the same  $[M - H]^-$  ion at  $m/z$  431. Compounds **10** and **11** showed a typical fragment of C-glycosides  $[M - H-120]^-$  at  $m/z$  311. In addition, their  $MS^2$  pattern corresponds to the vitexin and isovitexin fragmentation profiles, respectively [39]. The isomer **29** was generally assigned as apigenin-C-glucoside.

## 2.4. Identification of Quercetin Derivatives

Compounds **13**, **14**, **17**, **19**, **21**, **22**, **31**, and **33** are all characterized by the presence of the quercetin aglycone at  $m/z$  301. Compounds **13** and **17** showed parental ion at  $m/z$  477  $[M - H]^-$  with a NL of 176 Da  $[M - H-176]^-$  that is characteristic of the glucuronyl moiety. Compound **17** was identified by the GNPS assignment tool as quercetin-3-O-glucuronide, while its isomer, compound **13**, was tentatively identified as quercetin-O-glucuronide [41]. Compounds **14**, **22**, and **31** showed the same pseudomolecular ion at  $m/z$  463  $[M - H]^-$ , showing a NL of a glucoside moiety  $[M - H-162]^-$ . GNPS assigned compound **14** as isoquercitrin, while compounds **22** and **31** were tentatively assigned as hyperoside and quercetin-7-O-glucoside, respectively, by the comparison of their RT and  $MS^2$  fragments with previous studies [39][42]. Compound **19**,  $m/z$  505  $[M - H]^-$ , was identified by GNPS as Quercetin-3-O-glucose-6"-acetate, while its isomer compound **21** was generically assigned as quercetin-O-acetyl hexoside [41].

Compound **33**,  $m/z$  639  $[M - H]^-$ , showed fragments at  $m/z$  463 and 301 that correspond to the loss of glucuronyl and hexosyl moieties, respectively. Thus, on this evidence and coherently with a previous study [43], we assigned this compound as quercetin-O-glucuronide-O-hexoside.

## 2.5. Identification of Isorhamnetin Derivatives

Compounds **28** and **34** showed a fragment ion at  $m/z$  315 that is characteristic of the isorhamnetin aglycone after the NL of a glucuronyl  $[M - H-176]^-$  and hexose  $[M - H-162]^-$  moiety, respectively. Coherently with the literature, we assigned compound **28** as isorhamnetin3(7)-O-glucuronopyranoside and compound **34** as isorhamnetin-O-glucoside [44].

## 2.6. Other Flavonoids Assignment

Compounds **5**, **15**, **16**, **32**, **35**, and **36** were identified by GNPS as myricetin-3-O- $\beta$ -D-galactopyranoside, astragaloside, scoparin, 6-O-methylscutellarin, 4-(3,4-Dihydroxyphenyl)-5-beta-D-glucopyranosyloxy-7-methoxycoumarin, and isookanin-7-O-glucoside, respectively.

We could not assign any identification to compounds **3**, **7**, **12**, and **27**.

## 2.7. DGMG Assignment

Compound **37** was assigned as digalactosylmonoacylglycerol (DGMG) 18:3 by GNPS annotation tool. By comparison, compounds **38** and **39** were tentatively assigned as DGMG 20:5 and DGMG 16:2, respectively.

## 2.8. Antiviral Activity

In order to evaluate if leaf polyphenol extract had an antiviral potential, and in which stage of the viral infection it could act, we performed experiments in four conditions: (a) simultaneous addition of extract and virus to the cells (“co-treatment”); (b) extract firstly incubated with the virus and then added to the cells (“virus pre-treatment”); (c) extract added to the infected cells (“post-treatment”); and (d) cells treated before with the extract and then infected with the virus (“cell pre-treatment”). The tested range of extract concentrations was from 0.625 to 500  $\mu\text{g}/\text{mL}$  both for HSV-1 and SARS-CoV-2, which was used as a virus model for enveloped DNA and RNA viruses, respectively. The percentage of viral inhibition was calculated with respect to the untreated infected control (CTRL-). The reported antiviral activity was very similar for both viruses (**Figure 3** and **Figure 4**), indicating an early effect manifesting directly on the viral envelope. The extract was most effective when incubated with HSV-1 and SARS-CoV-2 upon addition to target cells (co-treatment, **Figure 3A** and **Figure 4A**) or with the virus (virus pre-treatment, **Figure 3B** and **Figure 4B**) prior to infection on the cell monolayer. No activity was registered when the extract was added after HSV-1 infection (post-treatment, **Figure 3C** and **Figure 4C**), while a slight antiviral effect was observed when cells were firstly treated with the extract and then infected (cell pre-treatment, **Figure 3D** and **Figure 4D**). In detail, leaf extract was able to completely inhibit HSV-1 replication in virus pre-treatment assay until a concentration of 10  $\mu\text{g}/\text{mL}$  was obtained but the virus resumed growing at 5  $\mu\text{g}/\text{mL}$ , though with less efficiency (**Figure 3B**). Instead, the antiviral activity of *V. vinifera* extract was slightly lower against SARS-CoV-2, as it was set at 80% at 10  $\mu\text{g}/\text{mL}$ . As HSV-1, no relevant inhibition was detected when the concentration of the extract was reduced to 5  $\mu\text{g}/\text{mL}$ .

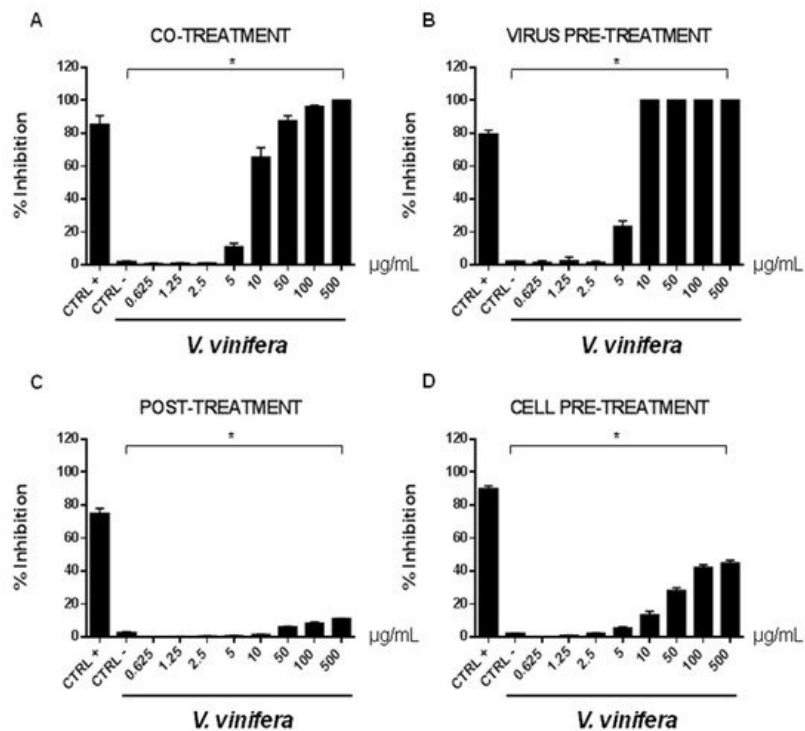


**Figure 3.** Antiviral effect (expressed as % of inhibition) of leaf extract ( $\mu\text{g}/\text{mL}$ ) against HSV-1 in different plaque reduction assays: (A) co-treatment; (B) virus pre-treatment; (C) post-treatment; (D) cell pre-treatment. The results presented were obtained from three independent experiments. Data are mean  $\pm$  SD. Statistical differences were analyzed via Student's t-test, a value of  $p \leq 0.05$  was considered significant, with \*  $p \leq 0.05$ .

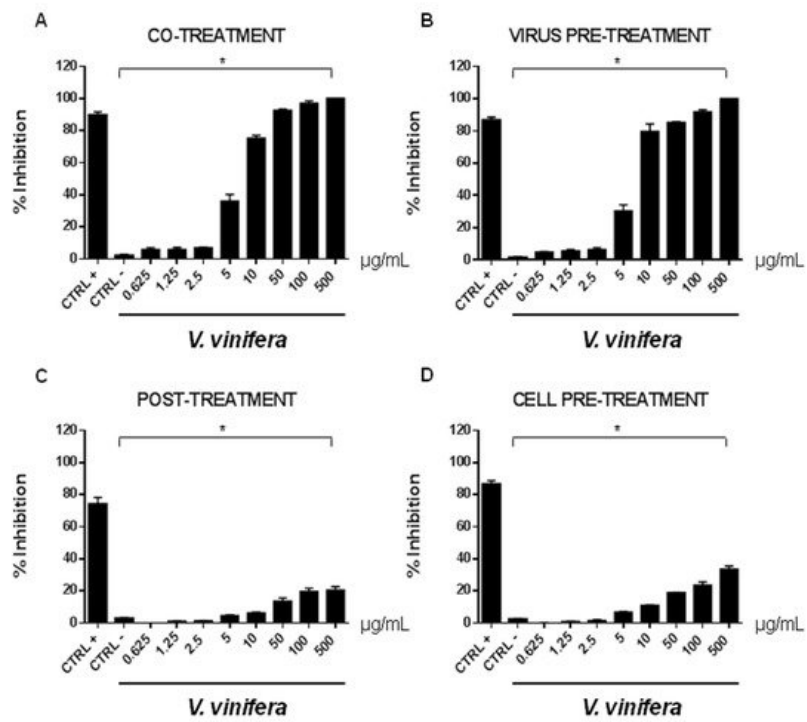


**Figure 4.** Antiviral effect (expressed as % of inhibition) of leaf extract ( $\mu\text{g/mL}$ ) against SARS-CoV-2 in different plaque reduction assays: **(A)** co-treatment; **(B)** virus pre-treatment; **(C)** post-treatment; **(D)** cell pre-treatment. The results presented were obtained from three independent experiments. Data are mean  $\pm$  SD. Statistical differences were analyzed via Student's t-test, a value of  $p \leq 0.05$  was considered significant, with \*  $p \leq 0.05$ .

The leaf extract definitely showed a stronger antiviral potential than Greco extract, which was used as a positive control (CTRL+) against HSV-1 and SARS-CoV-2 [11][45][46][47].

These data are very interesting and indicate that the leaf extract could act directly on viral particles, blocking the interaction with the cell membrane. To deepen the viral inactivation mechanism, another antiviral test was carried out, such as the attachment assay (**Figure 5** and **Figure 6**), by shifting the temperature during the infection at 4 °C.

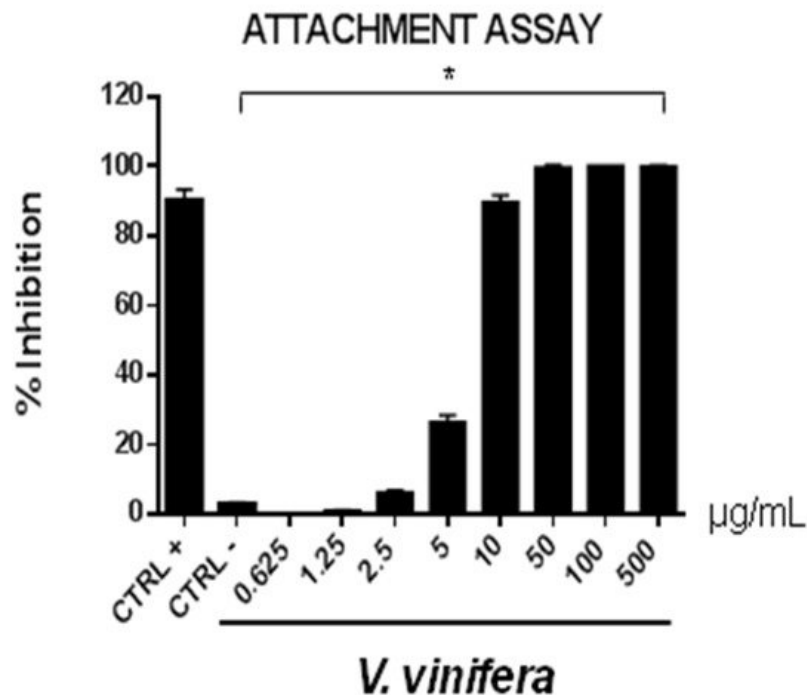


**Figure 5.** Early viral attachment assay of leaf extract ( $\mu\text{g/mL}$ ) against HSV-1. The antiviral activity is expressed as % of inhibition. The results presented were obtained from three independent experiments. Data are mean  $\pm$  SD. Statistical differences were analyzed via Student's t-test, a value of  $p \leq 0.05$  was considered significant, with \*  $p \leq 0.05$ .

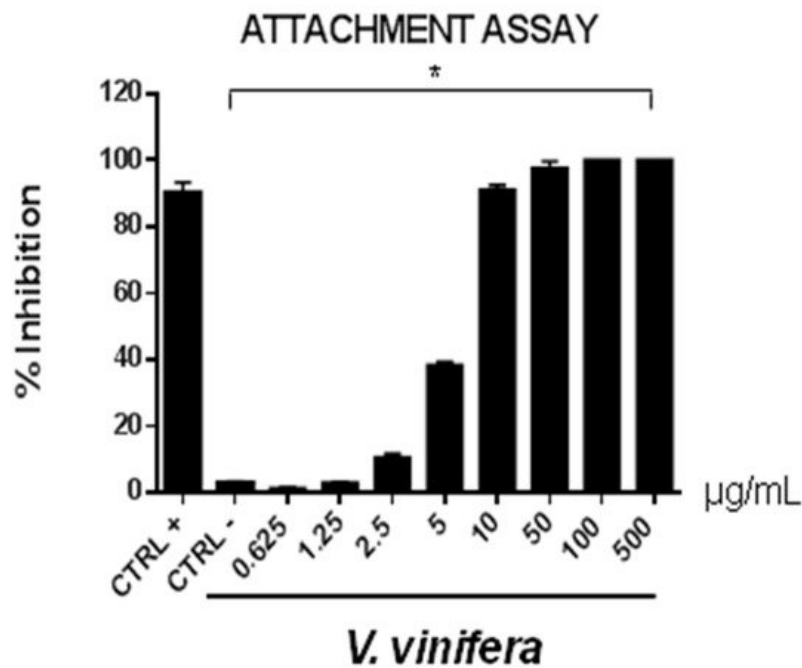


**Figure 6.** Early viral attachment assay of leaf extract (µg/mL) against SARS-CoV-2. The antiviral activity is expressed as % of inhibition. The results presented were obtained from three independent experiments. Data are mean ± SD. Statistical differences were analyzed via Student's t-test, a value of  $p \leq 0.05$  was considered significant, with \*  $p \leq 0.05$ .

The extract's inhibitory effects on virus-cell binding event revealed that it was able to block the attachment of both of the viruses into the host cell. It is most likely that leaf extract prevents the binding of viral envelope with the cell membrane and all the subsequent stages of infection by hindering some interacting site inside the viral glycoprotein deputed to the fusion, i.e., HSV-1 glycoprotein B and SARS-CoV-2 spike protein.

To validate data obtained by plaque assays, we analyzed the *V. vinifera* effect on expression genes involved in the viral infection (**Figure 7** and **Figure 8**).

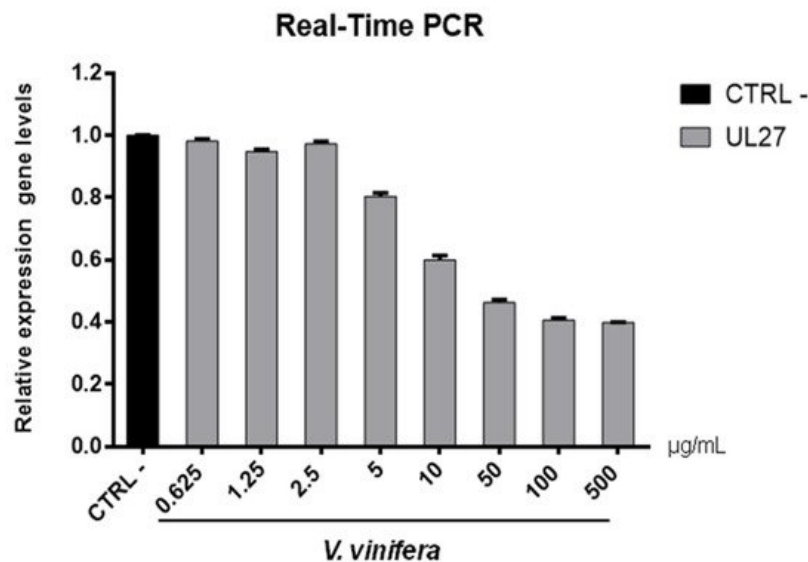


**Figure 7.** UL27 (glycoprotein B) gene expression analysis in Vero cells. *V. vinifera* leaf extract at 0.625, 1.25, 2.5, 5, 10, 50, 100, and 500 µg/mL was incubated with HSV-1 for 1 h and then, the mixture was added on Vero cells for another 1 h. After 2 days post-infection, RNA was extracted and Real-Time PCR was performed. Relative expression gene level was calculated with respect to CTRL-.

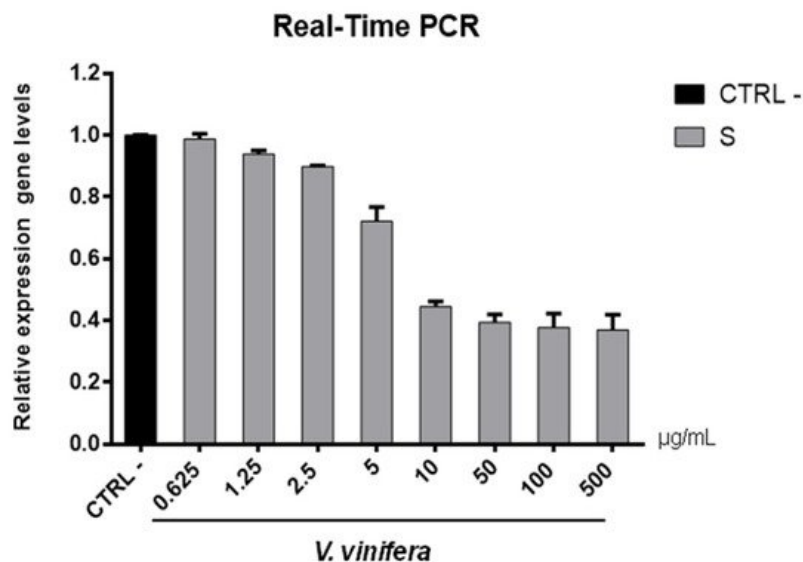


**Figure 8.** S gene expression analysis in Vero cells. *V. vinifera* leaf extract at 0.625, 1.25, 2.5, 5, 10, 50, 100, and 500 µg/mL was incubated with SARS-CoV-2 for 1 h and then the mixture was added on Vero cells for another 1 h. After 2 days post-infection, RNA was extracted, and Real-Time PCR was performed. Relative expression gene levels were calculated with respect to CTRL-.

Regarding the HSV-1 antiviral effect, UL27 gene, a late gene coding for the structural glycoprotein B (gB) was quantified via molecular assay (**Figure 7**). In brief, a virus pre-treatment assay was performed, as previously mentioned, and RNA was collected after 48 h post-infection. Results showed that the extract inhibited HSV-1 replication by blocking much of viral gene expression, which almost halved at a concentration of 10 µg/mL. The outcomes on the replication are in accordance with literature [48][49][50][51][52], demonstrating that the leaf extract had a virucidal action and could be used as a prophylactic treatment for herpetic infections. Anti-SARS-CoV-2 activity of *V. vinifera* leaf extract was also investigated through the spike protein (S) gene expression (**Figure 8**). S protein represents the anti-receptor inserted into the viral envelope essential to the attachment to the host cell via the human angiotensin-converting enzyme 2 (hACE2) receptor [53][54][55].

*V. vinifera* extract strongly reduced the S expression after SARS-CoV-2 infection until a concentration of 10 µg/mL was reached, and it resumed being expressed in a dose-dependent manner at lower concentrations. All together, these data indicated that *V. vinifera* leaf extract possesses a great antiviral and never previously investigated activity, which was reported against SARS-CoV-2. To date, the activity of flavonoids against SARS-CoV-2 has been analyzed with promising results in silico through bioinformatics approaches [56][57][58]; in addition, the activity of these molecules towards other coronaviruses, such as the Severe acute respiratory syndrome coronavirus (SARS-CoV) and Middle East Respiratory Syndrome Coronavirus (MERS), has been widely reported [59]. Altogether these results are noteworthy, although some phenolic compounds identified in the leaf extract are already reported as antiviral agents, such as quercetin which is currently under clinical trial [60]. This study focuses on the high anti-inflammatory ability of quercetin, effective in COVID-19 treatment, and its dosage depends on the type of treatment: 500 mg for prophylactic use and 1000 mg for curative treatment.

## 2.9. Cytotoxicity Evaluation

In order to complete the toxicological activity of leaf extract, *V. vinifera* was tested in colon, lung, breast, cardiomyocytes, hepatocyte cancer cells, and immortalized human keratinocyte cell line for 48 h at four different concentrations from 65 µg/mL to 500 µg/mL (**Figure 9A–F**). With respect to the known published anticancer effect of the grape, seeds, or peel of *V. vinifera* [61], the leaf extract did not induce any substantial variation in cell cancer viability. This different response, compared to that previously reported [62], could be explained by the different extraction methodologies or *V. vinifera* varieties used. These data suggest how this complex polyphenolic extract, in these conditions, was able to selectively act on a specific target, without altering other cellular mechanisms.

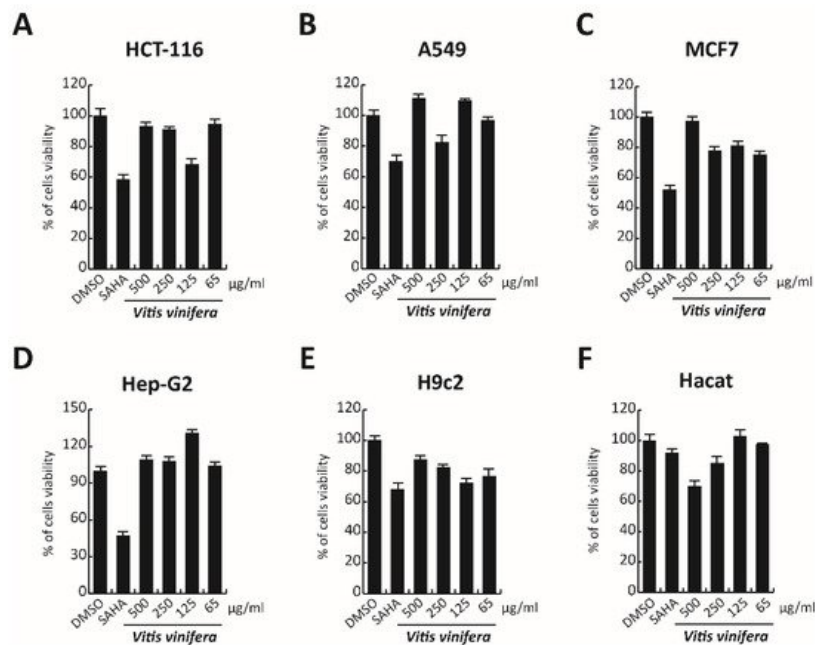


**Figure 9.** (A–F) Cell viability evaluation by MTT assay of HCT-116, A549, MCF7, cardiomyocytes, Hep-G2, and Hacat cells after treatment with *V. vinifera* for 48 h at 500, 250, 125, and 65 µg/mL. SAHA was used as a control at 5 µM for 24 h.

## References

- Rinaldi, A.; Villano, C.; Lanzillo, C.; Tamburrino, A., Jr.; Jourdes, M.; Teissedre, P.L.; Moio, L.; Frusciante, L.; Carputo, D.; Aversano, R. Metabolic and RNA profiling elucidates proanthocyanidins accumulation in Aglianico grape. *Food Chem.* 2017, 233, 52–59.
- Gratl, V.; Sturm, S.; Zini, E.; Letschka, T.; Stefanini, M.; Vezzulli, S.; Stuppner, H. Comprehensive polyphenolic profiling in promising resistant grapevine hybrids including 17 novel breeds in northern Italy. *J. Sci. Food Agric.* 2021, 101, 2380–2388.
- Sikuten, I.; Stambuk, P.; Andabaka, Z.; Tomaz, I.; Markovic, Z.; Stupic, D.; Maletic, E.; Kontic, J.K.; Preiner, D. Grapevine as a Rich Source of Polyphenolic Compounds. *Molecules* 2020, 25, 5604.
- Ju, Y.L.; Yue, X.F.; Min, Z.; Wang, X.H.; Fang, Y.L.; Zhang, J.X. VvNAC17, a novel stress-responsive grapevine (*Vitis vinifera* L.) NAC transcription factor, increases sensitivity to abscisic acid and enhances salinity, freezing, and drought tolerance in transgenic *Arabidopsis*. *Plant. Physiol. Biochem.* 2020, 146, 98–111.
- Batiha, G.E.; Beshbishy, A.M.; Ikram, M.; Mulla, Z.S.; El-Hack, M.E.A.; Taha, A.E.; Algammal, A.M.; Elewa, Y.H.A. The Pharmacological Activity, Biochemical Properties, and Pharmacokinetics of the Major Natural Polyphenolic Flavonoid: Quercetin. *Foods* 2020, 9, 374.
- Duan, J.; Zhan, J.C.; Wang, G.Z.; Zhao, X.C.; Huang, W.D.; Zhou, G.B. The red wine component ellagic acid induces autophagy and exhibits anti-lung cancer activity in vitro and in vivo. *J. Cell Mol. Med.* 2019, 23, 143–154.
- Saadaoui, N.; Weslati, A.; Barkaoui, T.; Khemiri, I.; Gadacha, W.; Souli, A.; Mokni, M.; Harbi, M.; Ben-Attia, M. Gastroprotective effect of leaf extract of two varieties grapevine (*Vitis vinifera* L.) native wild and cultivar grown in North of Tunisia against the oxidative stress induced by ethanol in rats. *Biomarkers* 2020, 25, 48–61.
- Fujita, K.; Aoki, Y.; Suzuki, S. Antidiabetic effects of novel cell culture established from grapevine, *Vitis vinifera* cv. Koshu. *Cytotechnology* 2018, 70, 993–999.
- Kim, H.Y.; Hong, M.H.; Yoon, J.J.; Kim, D.S.; Na, S.W.; Jang, Y.J.; Lee, Y.J.; Kang, D.G.; Lee, H.S. Protective Effect of *Vitis labrusca* Leaves Extract on Cardiovascular Dysfunction through HMGB1-TLR4-NFκB Signaling in Spontaneously Hypertensive Rats. *Nutrients* 2020, 12, 10.
- Li, L.; Zhang, M.; Zhang, S.; Cui, Y.; Sun, B. Preparation and Antioxidant Activity of Ethyl-Linked Anthocyanin-Flavanol Pigments from Model Wine Solutions. *Molecules* 2018, 23, 1066.
- Squillaci, G.; Zannella, C.; Carbone, V.; Minasi, P.; Folliero, V.; Stelitano, D.; Cara, F.L.; Galdiero, M.; Franci, G.; Morana, A. Grape Canes from Typical Cultivars of Campania (Southern Italy) as a Source of High-Value Bioactive Compounds: Phenolic Profile, Antioxidant and Antimicrobial Activities. *Molecules* 2021, 26, 2746.

12. Aliano-Gonzalez, M.J.; Richard, T.; Cantos-Villar, E. Grapevine Cane Extracts: Raw Plant Material, Extraction Methods, Quantification, and Applications. *Biomolecules* 2020, 10, 1195.
13. Sanchez, M.C.; Ribeiro-Vidal, H.; Esteban-Fernandez, A.; Bartolome, B.; Figuero, E.; Moreno-Arribas, M.V.; Sanz, M.; Herrera, D. Antimicrobial activity of red wine and oenological extracts against periodontal pathogens in a validated oral biofilm model. *BMC Complement. Altern Med.* 2019, 19, 145.
14. Lee, J.W.; Kim, Y.I.; Im, C.N.; Kim, S.W.; Kim, S.J.; Min, S.; Joo, Y.H.; Yim, S.V.; Chung, N. Grape Seed Proanthocyanidin Inhibits Mucin Synthesis and Viral Replication by Suppression of AP-1 and NF-kappaB via p38 MAPKs/JNK Signaling Pathways in Respiratory Syncytial Virus-Infected A549 Cells. *J. Agric. Food Chem.* 2017, 65, 4472–4483.
15. Zhang, X.Y.; Li, W.G.; Wu, Y.J.; Zheng, T.Z.; Li, W.; Qu, S.Y.; Liu, N.F. Proanthocyanidin from grape seeds potentiates anti-tumor activity of doxorubicin via immunomodulatory mechanism. *Int. Immunopharmacol.* 2005, 5, 1247–1257.
16. Lin, Y.S.; Chen, S.F.; Liu, C.L.; Nieh, S. The chemoadjuvant potential of grape seed procyanidins on p53-related cell death in oral cancer cells. *J. Oral Pathol. Med.* 2012, 41, 322–331.
17. Zykova, T.A.; Zhu, F.; Zhai, X.; Ma, W.Y.; Ermakova, S.P.; Lee, K.W.; Bode, A.M.; Dong, Z. Resveratrol directly targets COX-2 to inhibit carcinogenesis. *Mol. Carcinog.* 2008, 47, 797–805.
18. Sun, Q.; Prasad, R.; Rosenthal, E.; Katiyar, S.K. Grape seed proanthocyanidins inhibit the invasive potential of head and neck cutaneous squamous cell carcinoma cells by targeting EGFR expression and epithelial-to-mesenchymal transition. *BMC Complement. Altern. Med.* 2011, 11, 134.
19. Schlachterman, A.; Valle, F.; Wall, K.M.; Azios, N.G.; Castillo, L.; Morell, L.; Washington, A.V.; Cubano, L.A.; Dharmawardhane, S.F. Combined resveratrol, quercetin, and catechin treatment reduces breast tumor growth in a nude mouse model. *Transl. Oncol.* 2008, 1, 19–27.
20. Cai, W.; Chen, G.; Luo, Q.; Liu, J.; Guo, X.; Zhang, T.; Ma, F.; Yuan, L.; Li, B.; Cai, J. PMP22 Regulates Self-Renewal and Chemoresistance of Gastric Cancer Cells. *Mol. Cancer Ther.* 2017, 16, 1187–1198.
21. Borai, I.H.; Ezz, M.K.; Rizk, M.Z.; Aly, H.F.; El-Sherbiny, M.; Matloub, A.A.; Fouad, G.I. Therapeutic impact of grape leaves polyphenols on certain biochemical and neurological markers in AlCl<sub>3</sub>-induced Alzheimer's disease. *Biomed. Pharmacother.* 2017, 93, 837–851.
22. Di Meo, F.; Aversano, R.; Diretto, G.; Demurtas, O.C.; Villano, C.; Cozzolino, S.; Filosa, S.; Carputo, D.; Crispi, S. Anti-cancer activity of grape seed semi-polar extracts in human mesothelioma cell lines. *J. Funct. Foods* 2019, 61, 103515.
23. Radulescu, C.; Buruleanu, L.C.; Nicolescu, C.M.; Olteanu, R.L.; Bumbac, M.; Holban, G.C.; Simal-Gandara, J. Phytochemical Profiles, Antioxidant and Antibacterial Activities of Grape (*Vitis vinifera* L.) Seeds and Skin from Organic and Conventional Vineyards. *Plants* 2020, 9, 1470.
24. Al-Mousawi, A.H.; Al-Kaabi, S.J.; Albaghdadi, A.J.H.; Almulla, A.F.; Raheem, A.; Algon, A.A.A. Effect of Black Grape Seed Extract (*Vitis vinifera*) on Biofilm Formation of Methicillin-Resistant *Staphylococcus aureus* and *Staphylococcus haemolyticus*. *Curr Microbiol* 2020, 77, 238–245.
25. Pavic, V.; Kujundzic, T.; Kopic, M.; Jukic, V.; Braun, U.; Schwander, F.; Drenjancevic, M. Effects of Defoliation on Phenolic Concentrations, Antioxidant and Antibacterial Activity of Grape Skin Extracts of the Varieties Blaufrankisch and Merlot (*Vitis vinifera* L.). *Molecules* 2019, 24, 2444.
26. Olejar, K.J.; Ricci, A.; Swift, S.; Zujovic, Z.; Gordon, K.C.; Fedrizzi, B.; Versari, A.; Kilmartin, P.A. Characterization of an Antioxidant and Antimicrobial Extract from Cool Climate, White Grape Marc. *Antioxidants* 2019, 8, 232.
27. Santella, B.; Folliero, V.; Pirofalo, G.M.; Serretiello, E.; Zannella, C.; Moccia, G.; Santoro, E.; Sanna, G.; Motta, O.; De Caro, F.; et al. Sepsis-A Retrospective Cohort Study of Bloodstream Infections. *Antibiotics* 2020, 9, 851.
28. Zannella, C.; Shinde, S.; Vitiello, M.; Falanga, A.; Galdiero, E.; Fahmi, A.; Santella, B.; Nucci, L.; Gasparro, R.; Galdiero, M.; et al. Antibacterial Activity of Indolicidin-Coated Silver Nanoparticles in Oral Disease. *Appl. Sci.* 2020, 10, 1837.
29. Andelkovic, M.; Radovanovic, B.; Andelkovic, A.M.; Radovanovic, V. Phenolic Compounds and Bioactivity of Healthy and Infected Grapevine Leaf Extracts from Red Varieties Merlot and Vranac (*Vitis vinifera* L.). *Plant Foods Hum. Nutr.* 2015, 70, 317–323.
30. Rodríguez Vaquero, M.J.; Alberto, M.R.; Manca de Nadra, M.C. Influence of phenolic compounds from wines on the growth of *Listeria monocytogenes*. *Food Control.* 2007, 18, 587–593.
31. Papadopoulou, C.; Soulti, K.; Roussis, I. Potential Antimicrobial Activity of Red and White Wine Phenolic Extracts against Strains of *Staphylococcus aureus*, *Escherichia coli* and *Candida albicans*. *Food Technol. Biotechnol.* 2005, 43, 41–46.

32. Sukovic, D.; Knezevic, B.; Gasic, U.; Sredojevic, M.; Ciric, I.; Todic, S.; Mutic, J.; Tesic, Z. Phenolic Profiles of Leaves, Grapes and Wine of Grapevine Variety Vranac (*Vitis vinifera* L.) from Montenegro. *Foods* 2020, 9, 138.
33. Hassan, W.H.B.; Abdelaziz, S.; Al Yousef, H.M. Chemical Composition and Biological Activities of the Aqueous Fraction of *Parkinsonia aculeata* L. Growing in Saudi Arabia. *Arab. J. Chem.* 2019, 12, 377–387.
34. Pluskal, T.; Castillo, S.; Villar-Briones, A.; Oresic, M. MZmine 2: Modular framework for processing, visualizing, and analyzing mass spectrometry-based molecular profile data. *BMC Bioinform.* 2010, 11, 395.
35. Wang, M.; Carver, J.J.; Phelan, V.V.; Sanchez, L.M.; Garg, N.; Peng, Y.; Nguyen, D.D.; Watrous, J.; Kapono, C.A.; Luzzatto-Knaan, T.; et al. Sharing and community curation of mass spectrometry data with Global Natural Products Social Molecular Networking. *Nat. Biotechnol.* 2016, 34, 828–837.
36. Vitale, G.A.; Sciarretta, M.; Cassiano, C.; Buonocore, C.; Festa, C.; Mazzella, V.; Nunez Pons, L.; D'Auria, M.V.; de Pascale, D. Molecular Network and Culture Media Variation Reveal a Complex Metabolic Profile in *Pantoea* cf. *eucria* D2 Associated with an Acidified Marine Sponge. *Int. J. Mol. Sci.* 2020, 21, 6307.
37. Brito, A.; Ramirez, J.E.; Areche, C.; Sepulveda, B.; Simirgiotis, M.J. HPLC-UV-MS profiles of phenolic compounds and antioxidant activity of fruits from three citrus species consumed in Northern Chile. *Molecules* 2014, 19, 17400–17421.
38. Geng, P.; Sun, J.; Zhang, M.; Li, X.; Harnly, J.M.; Chen, P. Comprehensive characterization of C-glycosyl flavones in wheat (*Triticum aestivum* L.) germ using UPLC-PDA-ESI/HRMS(n) and mass defect filtering. *J. Mass Spectrom.* 2016, 51, 914–930.
39. Elsadig Karar, M.; Kuhnert, N. UPLC-ESI-Q-TOF-MS/MS Characterization of Phenolics from *Crataegus monogyna* and *Crataegus laevigata* (Hawthorn) Leaves, Fruits and their Herbal Derived Drops (*Crataegutt Tropfen*). *J. Chem. Biol. Ther.* 2016, 1, 102.
40. Spinola, V.; Llorent-Martinez, E.J.; Castilho, P.C. Antioxidant polyphenols of Madeira sorrel (*Rumex maderensis*): How do they survive to in vitro simulated gastrointestinal digestion? *Food Chem.* 2018, 259, 105–112.
41. Dueñas, M.; Mingo-Chornet, H.; Pérez-Alonso, J.; Di Paola, R.; Gonzalez-paramas, A.M.; Santos Buelga, C. Preparation of quercetin glucuronides and characterization by HPLC–DAD–ESI/MS. *Eur. Food Res. Technol.* 2008, 227, 1069–1076.
42. Chen, G.; Li, X.; Saleri, F.; Guo, M. Analysis of Flavonoids in *Rhamnus davurica* and Its Antiproliferative Activities. *Molecules* 2016, 21, 1275.
43. Roriz, C.L.; Barros, L.; Carvalho, A.M.; Santos-Buelga, C.; Ferreira, I.C. Scientific validation of synergistic antioxidant effects in commercialised mixtures of *Cymbopogon citratus* and *Pterospartum tridentatum* or *Gomphrena globosa* for infusions preparation. *Food Chem.* 2015, 185, 16–24.
44. Marczak, Ł.; Znajdek-Awiżeń, P.; Bylka, W. The Use of Mass Spectrometric Techniques to Differentiate Isobaric and Isomeric Flavonoid Conjugates from *Axyris amaranthoides*. *Molecules* 2016, 21, 1229.
45. World Health Organization. Coronavirus Disease (COVID-19) Pandemic; World Health Organization: Geneva, Switzerland, 2020.
46. Chianese, A.; Santella, B.; Ambrosino, A.; Stelitano, D.; Rinaldi, L.; Galdiero, M.; Zannella, C.; Franci, G. Oncolytic Viruses in Combination Therapeutic Approaches with Epigenetic Modulators: Past, Present, and Future Perspectives. *Cancers* 2021, 13, 2761.
47. Falanga, A.; Del Genio, V.; Kaufman, E.A.; Zannella, C.; Franci, G.; Weck, M.; Galdiero, S. Engineering of Janus-Like Dendrimers with Peptides Derived from Glycoproteins of Herpes Simplex Virus Type 1: Toward a Versatile and Novel Antiviral Platform. *Int. J. Mol. Sci.* 2021, 22, 6488.
48. Monda, V.; Valenzano, A.; Monda, M. Modifications of Activity of Autonomic Nervous System, and Resting Energy Expenditure in Women Using Hormone-Replacement Therapy. *Biol. Med.* 2016, 8, 1.
49. Schiattarella, A.; Riemma, G.; La Verde, M.; Franci, G.; Chianese, A.; Fasulo, D.; Fichera, M.; Gallo, P.; De Franciscis, P. Polycystic ovary syndrome and probiotics: A natural approach to an inflammatory disease. *Curr. Womens Health Rev.* 2021, 17, 14–20.
50. Russo, M.; Moccia, S.; Spagnuolo, C.; Tedesco, I.; Russo, G.L. Roles of flavonoids against coronavirus infection. *Chem. Biol. Interact.* 2020, 328, 109211.
51. Urmenyi, F.G.; Saraiva, G.D.; Casanova, L.M.; Matos, A.D.; de Magalhaes Camargo, L.M.; Romanos, M.T.; Costa, S.S. Anti-HSV-1 and HSV-2 Flavonoids and a New Kaempferol Triglycoside from the Medicinal Plant *Kalanchoe daigremontiana*. *Chem. Biodivers.* 2016, 13, 1707–1714.
52. Abdallah, H.M.; El-Halawany, A.M.; Sirwi, A.; El-Araby, A.M.; Mohamed, G.A.; Ibrahim, S.R.M.; Koshak, A.E.; Asfour, H.Z.; Awan, Z.A. Repurposing of Some Natural Product Isolates as SARS-COV-2 Main Protease Inhibitors via In Vitro

53. Conceicao, C.; Thakur, N.; Human, S.; Kelly, J.T.; Logan, L.; Bialy, D.; Bhat, S.; Stevenson-Leggett, P.; Zagrajek, A.K.; Hollinghurst, P.; et al. The SARS-CoV-2 Spike protein has a broad tropism for mammalian ACE2 proteins. *PLoS Biol.* 2020, *18*, e3001016.
54. Hoffmann, M.; Kleine-Weber, H.; Schroeder, S.; Kruger, N.; Herrler, T.; Erichsen, S.; Schiergens, T.S.; Herrler, G.; Wu, N.H.; Nitsche, A.; et al. SARS-CoV-2 Cell Entry Depends on ACE2 and TMPRSS2 and Is Blocked by a Clinically Proven Protease Inhibitor. *Cell* 2020, *181*, 271–280.e8.
55. Zhao, P.; Praissman, J.L.; Grant, O.C.; Cai, Y.; Xiao, T.; Rosenbalm, K.E.; Aoki, K.; Kellman, B.P.; Bridger, R.; Barouch, D.H.; et al. Virus-Receptor Interactions of Glycosylated SARS-CoV-2 Spike and Human ACE2 Receptor. *Cell Host Microbe* 2020, *28*, 586–601.e6.
56. Pandey, P.; Khan, F.; Rana, A.K.; Srivastava, Y. A drug repurposing approach towards elucidating the potential of flavonoids as COVID-19 spike protein inhibitors. *Biointerface Res. Appl. Chem.* 2021, *11*, 8482–8501.
57. Mouffouk, C.; Mouffouk, S.; Mouffouk, S.; Hambaba, L.; Haba, H. Flavonols as potential antiviral drugs targeting SARS-CoV-2 proteases (3CL(pro) and PL(pro)), spike protein, RNA-dependent RNA polymerase (RdRp) and angiotensin-converting enzyme II receptor (ACE2). *Eur. J. Pharmacol.* 2021, *891*, 173759.
58. Jain, A.S.; Sushma, P.; Dharmashekar, C.; Beelagi, M.S.; Prasad, S.K.; Shivamallu, C.; Prasad, A.; Syed, A.; Marraiki, N.; Prasad, K.S. In silico evaluation of flavonoids as effective antiviral agents on the spike glycoprotein of SARS-CoV-2. *Saudi J. Biol. Sci.* 2021, *28*, 1040–1051.
59. Taban, A.K.; Süntar, İ. An Overview on Flavonoids as Potential Antiviral Strategies against Coronavirus Infections. *Gazi Med. J.* 2020.
60. Effect of Quercetin on Prophylaxis and Treatment of COVID-19. Available online: <https://clinicaltrials.gov/ct2/show/NCT04377789> (accessed on 28 June 2021).
61. Grace Nirmala, J.; Evangeline Celsia, S.; Swaminathan, A.; Narendhirakannan, R.T.; Chatterjee, S. Cytotoxicity and apoptotic cell death induced by *Vitis vinifera* peel and seed extracts in A431 skin cancer cells. *Cytotechnology* 2018, *70*, 537–554.
62. Abed, A.; Harb, J.; Khasib, S.; Saad, B. In vitro assessment of cytotoxic, antioxidant and antimicrobial activities of leaves from two grape varieties collected from arid and temperate regions in Palestine. *QSci. Connect* 2015, *2015*, 4.